STUDY OF FLOW OF SYNTHETIC BASED DRILLING FLUIDS UNDER ELEVATED PRESSURE AND TEMPERATURE (EPET) CONDITIONS

INVESTIGATOR: Barkim DEMIRDAL
COMPLETION DATE: Summer 2000
SPONSORED BY: ACTF JIP and DOE

OBJECTIVE

1. To investigate the rheological behavior of synthetic based drilling fluids by using Advanced Cutting Transport Facility (ACTF) as a pipe viscometer under elevated pressure and temperature (EPET) conditions
2. To verify available empirical and semi-empirical turbulent flow models for estimating turbulent pressure losses by using experimental data
3. To develop a computer program that predicts parasitic pressure losses for various flow rates, composition of mud and wellbore geometry during the flow of synthetic based drilling fluid

PAST WORK

- Literature review of relevant works on synthetic based drilling fluid rheology; pressure loss calculations in actual wells and compositions to define flow of synthetic based drilling fluids
- Literature review of work done to define turbulent flow of Newtonian and non-Newtonian fluids in pipes and annuli
- The calibration of the flow loop and the data acquisition devices

PRESENT WORK

- Experiments of applying pressure to the system and measuring the response of data acquisition system to the pressure increase
- ACTF flow loop is modified for providing flow in pipes and drilling section connected in series and/or parallel
- Literature review on the relevant work on characterizing the rheology of an emulsion fluid under high temperature and pressure.
- Review of Newtonian and non-Newtonian fluids' turbulent flow models

FUTURE WORK

- Adding heat capacity to the system
- Experimental study of synthetic based drilling fluids under elevated pressure and temperature in the ACTF loop, and at high pressure and temperature in the HP-HT rotational viscometer
- Comparison of experimental data with pressure losses obtained from theoretical equations and development of a computational tool that calculates bottom hole pressure and equivalent circulating density

INTRODUCTION

Oil based drilling fluids are preferable for better shale inhibition, wellbore stabilization and lubrication when compared with water based drilling fluids. However, starting in the 1980's, it was understood that oil based drilling fluids, even the low toxicity mineral oils, did not biodegrade adequately in a cuttings pile to allow degradation of oil and recovery of the sea bed within an acceptable period of time. Increasing legislative restrictions on the discharge of cuttings contaminated with mineral oil resulted in the development of new drilling fluids that are more acceptable to the environment, and able to achieve the properties of oil base muds. In addition to being environmentally safe, synthetic based drilling fluids also avoid some disadvantages encountered in deep and ultra-deep wells drilled with water base muds. These include, gas hydrate formation in blow-out preventers and hole cleaning problems in large diameter riser sections. In addition to reducing these effects, lessen solubility of gas in synthetic based drilling fluids allows quicker detection of gas influx to the system so that a well can be controlled more easily.

Hydraulic design calculations and optimization programs based on these hydraulic calculations have vital importance for achieving either high ROP and/or low cost. Parasitic (frictional) pressure losses is one of the key parameters to determine ECD (Equivalent Circulating Densities) and pump pressures, which in turn affects surge/swab pressures while tripping, sizing of mud pumps, well control and general well planning. Parasitic pressure losses can be obtained either by using electronic devices and measuring the actual pressure of the system while drilling (Pressure While Drilling (PWD) and Measurement While Drilling (MWD) tools) or by using pressure loss equations derived for flow of non-Newtonian fluid flow in pipes and annuli.

The successful prediction of frictional pressure losses by using these equations depends on the accurate representation of the drilling fluid rheology. Usually, rheology of the fluid is determined under ambient conditions and extrapolated to downhole conditions. However, it is known that rheology of drilling fluids is influenced by many parameters (temperature, pressure, shear history, composition of the drilling fluid) and show different properties under high or low shear rates. Since synthetic based drilling fluids are more sensitive to temperature and pressure than any other type of drilling fluid, a detailed study of their high pressure and high temperature behavior is needed to understand how differences in rheological characteristics migh affect hydraulics. This part of the research will be conducted both by using an HPHT rotational viscometer and a pipeline viscometer section of the Advanced Cutting Transport Facility (ACTF). The effect of cyclical variations in temperature and pressure on the fluid's rheology can be observed by comparing closed pipe-loop viscometer data with HPHT rotational viscometer data.

After determining the rheological model of the synthetic fluids under high pressure and temperature, the experimental frictional losses will be compared with theoretical pressure losses derived by previous investigators to see whether these equations can be used to determine pressure losses efficiently. Friction factor vs. Reynolds Number charts will be obtained for the particular mud system under investigation and the effect of drag reducers on pressure losses will be determined. In this way, applicability of laminar flow based semi-empirical or empirical pressure loss equations for turbulent flow conditions will be determined and necessary changes will be made to obtain more accurate predictions.

To do this analysis, the ACTF Loop will be used as a pipe viscometer. It has a wide range of pressure and temperature with upper limits of 1400 psig and 200 ^{o}F. The flowrate can be increased up to 300 gpm which allows high shear rates comparable to those encountered in a drill pipe during drilling operations. Fann Model 70 Viscometer will also be used as HPHT rotational viscometer to determine HPHT rheological properties of the mud under investigation.

SCOPE OF THE PROJECT

Experimental analysis of synthetic based drilling fluids under elevated pressures and elevated temperatures will be carried both by using an HPHT rotational viscometer and the ACTF Loop located on the North Campus of The University of Tulsa. Rheological characterization of the fluids obtained by rotational viscometer and pipe viscometer will be compared. Pressure losses obtained by the experiments will be compared with empirical and semi-empirical equations to examine the applicability of laminar flow theory for turbulent flow. The Friction factor (f) vs. Reynolds number for a given fluid will be plotted. The effect of drag reducers on the pressure losses and rheology of the synthetic drilling fluid will be analyzed. A computational tool that calculates frictional pressure losses and equivalent circulating density for a given fluid system will be developed.

THEORY OF TURBULENT FLOW OF NON-NEWTONIAN FLUIDS:

Turbulent Flow of Non-Newtonian Fluids in Pipes:

The behavior of a flowing fluid is determined by the flow regime, which in turn has a direct effect on the ability of that fluid to perform its basic functions. Flows are generally defined as either laminar or turbulent. Between them, there is a transition region, where a fluid has both laminar and turbulent characteristics. This region is controlled by the relative importance of viscous forces and inertial forces in the flow. *Laminar flow* is flow in which fluid layers moves parallel to the walls of the flow channel and each other in smooth lines. This type of flow can be represented by the Navier-Stokes equations. On the other hand, flow that does not satisfy the Navier-Stokes equations for a viscous fluid that flows with relatively high Reynolds numbers are often termed *turbulent flow*. In turbulent flow both the velocities and pressure gradients are fluctuating and these fluctuations are random. To define mean velocity, temperature distributions and pressure losses in turbulent systems, either semi-empirical and empirical theories or application of statistical mechanics should be used. The latter is beyond the aim of this research, so this study will deal with semi-empirical and empirical theories that are developed to define turbulent flow systems.

Early investigators made several attempts to define turbulent flow of non-Newtonian fluids. They assumed that, the non-Newtonian fluid in laminar flow as effectively Newtonian in turbulent flow, any variation in apparent viscosity under turbulent conditions being disregarded. Thus non-Newtonian friction data for tubes were correlated on the conventional friction factor-Reynolds Number curve for turbulent Newtonian fluids, using variety of terms for viscosity in the Reynolds number.

Caldwell and Babbitt [1] proposed that apparent viscosity of Bingham-Plastic fluids is the viscosity of the dispersion medium, which is water in the case of water base drilling fluids.

Hedstrom and Weltmann [2] introduce the concept of plastic viscosity (η) to use in the N_{Re} equation for Bingham-Plastic fluids.

For power-law fluids in turbulent flow, Weltmann [3] proposed an apparent viscosity at the pipe wall, $\mu_a = g_c \tau_w / (-du/dr)$, and that N_{Re} is a function of fluid behavior index, *n*.

Alves, Boucher and Pigford [4] introduced a turbulent viscosity that can be obtained by using *f* vs. N_{Re} curves that were sketched for Newtonian fluids.

Extensive theoretical and experimental studies on turbulent flow of non-Newtonian fluids were carried by Metzner and Reed [5], and Dodge and Metzner [6]. It is known from power-law fluids that the relation between wall shear stress, $\tau_{r=R}$, and wall shear rate, 8V/D, at laminar flow can be given as;

$$\left(\tau_{rx}\right)_{r=R} = \tau_w = K'\left(\frac{8V}{D}\right)^{n'} \quad \text{.....(1)}$$

The Fanning Friction factor is defined as;

$$f = \frac{g_c\left(\frac{D\Delta P}{4L}\right)}{\frac{\rho V^2}{2}} = \frac{g_c \tau_w}{\frac{\rho V^2}{2}} \quad \text{.....(2)}$$

Substituting Equation (1) into Equation (2);

$$f = \frac{2g_c}{\rho V^2} K'\left(\frac{8V}{D}\right)^{n'} = \frac{16\gamma}{D^{n'} V^{2-n'} \rho} \quad \text{.....(3)}$$

For the case of laminar, Newtonian flow;

$$f = \frac{16\mu}{DV\rho} = \frac{16}{N_{\mathrm{Re}}} \quad \text{.....(4)}$$

At this point they assume that the Power-Law Reynolds number can be derived from Newtonian fluid by equating (3) and (4) as follows

$$N_{\mathrm{Re}} = \frac{D^{n'}V^{2-n'}\rho}{\gamma} \quad \text{.....(5)}$$

The above derivation shows that all fluids which are not time dependent must obey conventional Newtonian friction factor vs. Reynolds Number when flow is laminar. As a next step, they predicted the velocity elements of flow in turbulent, laminar and buffer zones. For fully-turbulent flow of a non-Newtonian fluid in a smooth tube, local velocity in the direction of flow is a function of;

$$u = f\left(R, \rho, \tau_w g_c, K, n, y\right) \quad \text{.....(6)}$$

For the flow within the wall region, velocity is independent of the radius of the pipe in the laminar boundary layer, the transition zone and the outermost turbulent core, so that;

$$u = f\left(\rho, \tau_w g_c, K, n, y\right) \quad \text{.....(7)}$$

For the velocity defect, which is the difference between the maximum local velocity in the center of the pipe (u_m) and local velocity (u), it can be stated that the effect of viscosity is negligible in turbulent fluctuations that occur in the core. For non-Newtonian fluids, velocity defect (u_m-u) is independent of K but dependent on *n*.

$$u_m - u = f\left(\tau_w g_c, \rho, R, y, n\right) \quad \text{.....(8)}$$

Above three relations are solved by using the Buckingham's Pi Theorem;

A general function for u/u^* at any radial location,

$$\frac{u}{u^*} = f_1\left(Z, \xi, n\right) \quad \text{.....(9)}$$

where

$$Z = \frac{R^n \rho \left(u^*\right)^{2-n}}{K} \quad \text{.....(10)}$$

$$u^* = \sqrt{\frac{\tau_w g_c}{\rho}} \quad \text{.....(11)}$$

$$\xi = \frac{y}{R} \quad \text{.....(12)}$$

A general function for u/u^* within the wall region,

$$\frac{u}{u^*} = f_2\left(Z\xi^n, n\right) \quad \text{.....(13)}$$

A general function for $(u_m-u)/u^*$ in the turbulent core,

$$\frac{u_m - u}{u^*} = f_3\left(\xi, n\right) \quad \text{.....(14)}$$

A general function for $(u_m-V)/u^*$,

$$\frac{u_m - V}{u^*} = P_n \quad \text{.....(15)}$$

Assuming that transition and laminar layers are thin for Newtonian fluids and even thinner for pseudoplastic fluids transition and laminar layers are neglected.

Equation (9) for the center of the pipe can be written as:

$$\frac{u_m}{u^*} = f_1\left(Z, 1, n\right) = F_1\left(Z, n\right) \quad \text{.....(16)}$$

or from Equation (15),

$$\frac{u_m}{u^*} = P_n + \frac{V}{u^*} \quad \text{.....(17)}$$

Friction factor defined in Equation (2) can be written in terms of u^* as,

$$V\sqrt{\frac{\rho}{\tau_w g_c}} = \frac{V}{u^*} = \sqrt{\frac{2}{f}} \quad \text{.....(18)}$$

Combining Equation (17) and (18),

$$\sqrt{\frac{2}{f}} = F_1(Z,n) - P_n \quad \text{.....(19)}$$

It was shown that, at the outer part of the turbulent core, equation (13) for the wall region and equation (14) for the turbulent core are both assumed to be valid. Thus,

$$\frac{u}{u^*} = \frac{u_m}{u^*} - \frac{u_m - u}{u^*} \quad \text{.....(20)}$$

or in terms of the functions we use to define these parameters,

$$f_2(Z\xi^n, n) = F_1(Z,n) - f_3(\xi^n, n) \quad \text{.....(21)}$$

Considering the above relationship for a fixed value of *n*,

$$f_{2n}(Z\xi^n) = F_{1n}(Z) - f_{3n}(\xi^n) \quad \text{.....(22)}$$

Specific form of $F_{1n}(Z)$ can be determined by a procedure involving partial differentiation of equation (22) with respect to Z and ξ^n. At the end of this derivation, they come up with:

$$\frac{u_m}{u^*} = F_{1n}(Z) = A_n \ln Z + Bn \quad \text{.....(23)}$$

where A_n and B_n are regarded as functions of n. Dodge and Metzner [6] states that, equation (23) does not contain ξ, and they therefore conclude that the equation is independent of the location and width of the overlapping region. Substituting equation (23) in to equation (19),

$$\sqrt{\frac{2}{f}} = A_n \ln Z + B_n - P_n \quad \text{.....(24)}$$

After determining the general relation for the friction factor, a relation between the friction factor and the Reynolds number is obtained by replacing Z and dividing by √2 as,

$$\sqrt{\frac{1}{f}} = 1.628A_n \log\left[N^o{}_{\mathrm{Re}}\left(f\right)^{1-n/2}\right] - 0.4901A_n\left(1+\frac{n}{2}\right) + \frac{B_n - P_n}{\sqrt{2}} \quad \text{.....(25)}$$

or

$$\sqrt{\frac{1}{f}} = A_{1n} \log\left[N^o{}_{\mathrm{Re}}\left(f\right)^{1-n/2}\right] + C_n \quad \text{.....(26)}$$

where:

$$N^o{}_{\mathrm{Re}} = \frac{D^n V^{2-n}\rho}{K} \quad \text{.....(27)}$$

$$A_{1n} = 1.628A_n \quad \text{.....(28)}$$

$$C_n = -0.491A_n\left(1+\frac{n}{2}\right) + \frac{B_n - P_n}{\sqrt{2}} \quad \text{.....(29)}$$

Metzner and Reed's [5], and Dodge and Metzner's [6] assumption is based on using *K'* and *n'* parameters obtained under laminar flow within the wall region, to predict rheological constants *K* and *n*. To do this, the generalized Reynolds number for Power_law fluids should be defined as;

$$\left(N_{\mathrm{Re},gen}\right)_{power-law} = \frac{D^n V^{2-n}\rho}{8^{n-1}K\left[\left(3n+1\right)/4n\right]^n} \quad \text{.....(30)}$$

or

$$N^o{}_{\mathrm{Re}} = \frac{1}{8}\left(\frac{6n+2}{n}\right)^n (N_{Re,gen}) \quad \text{.....(31)}$$

Thus, the friction factor can be expressed in terms of a generalized Reynolds number as;

$$\sqrt{\frac{1}{f}} = A_{1n} \log\left[N_{\mathrm{Re},gen}\left(f\right)^{1-n'/2}\right] + C_n' \quad \text{.....(32)}$$

where

$$C_n^{'} = A_{1n} \log\left[\frac{1}{8}\left(\frac{6n^{'}+2}{n'}\right)^{n'}\right] + C_n \quad \text{.....(33)}$$

In the last equation, expression A_{1n}, $C_n^{'}$, $n^{'}$ can be determined experimentally. The experimental measurements of Dodge and Metzner [6] include extensive data on Power-Law fluids which were use to obtain the following empirical relationships;

$$A_{1n} = \frac{4.0}{(n')^{0.75}} \quad \text{.....(34)}$$

$$C_n^{'} = \frac{-.40}{(n^{'})^{1.2}} \quad \text{.....(35)}$$

Inserting these relations to equation (16),

$$\sqrt{\frac{1}{f}} = \frac{4}{(n')^{0.75}} \log\left[N_{\mathrm{Re},gen}(f)^{1-n/2}\right] - \frac{0.40}{(n')^{1.2}} \quad \text{.....(36)}$$

Dodge and Metzner [6] proposed another model for non-Newtonian fluid in turbulent flow. They derived a turbulent flow correlation by introducing apparent viscosity in Reynolds Number and by combining laminar flow equations for Newtonian and Power-Law fluids.

Another approach for predicting resistance to turbulent flow was introduced by Tomita [7]. He used similarity criteria and Prandtl's mixing length theory to define laminar and turbulent flow in Bingham Plastic and Power-Law fluids. First, by using similarity considerations, expressions for f and the Reynolds Number for Bingham Plastics in laminar flow is determined as;

$$f_B = \frac{D\Delta P g_c}{2\rho L V^2 (1-c)} \quad \text{.....(37)}$$

and

$$N_{\mathrm{Re},B} = \frac{DV\rho}{\eta}\frac{(1-c)(c^4-4c+3)}{3} \quad \text{.....(38)}$$

where c can be obtained from known values of V, R, τ_y and η that are obtained for laminar flow by using the following relation:

$$V = \frac{Rg_c\tau_y}{\eta}\left(\frac{c^4-4c+3}{12c}\right) \quad \text{.....(39)}$$

This relation was obtained by balancing between shear and pressure forces acting on Bingham Plastic fluids in steady laminar flow. That is why Tomita called his model "Considering the turbulent flow as laminar flow". After applying Prandtl's mixing length theory to obtain the relation between f_B and $N_{Re,B}$, and by using laminar flow expressions with numerical constants obtained for Newtonian fluids, the result is;

$$\sqrt{\frac{1}{f}} = 4\log\left(N_{\mathrm{Re},B}\sqrt{f_B}\right) - 0.40 \quad \text{.....(40)}$$

Using similarity considerations of laminar flow in smooth tubes for the Power-Law fluids results in,

$$f_p = \frac{2D\Delta Pg_c(2n+1)}{3L\rho V^2(3n+1)} \quad \text{.....(41)}$$

and

$$N_{\mathrm{Re},P} = \frac{6[(3n+1)/n]^n}{2^n[(2n+1)/n]}\frac{D^nV^{2-n}\rho}{K} \quad \text{.....(42)}$$

After, again applying Prandtl's mixing length theory, and experimentally obtaining numerical constants for Newtonian fluids flowing through pipes with diameters ranging from 2" to 1/8" the following equation is obtained:

$$\sqrt{\frac{1}{f_P}} = 4\log\left(N_{\mathrm{Re},P}\sqrt{f_p}\right) - 0.40 \quad \text{.....(43)}$$

Although it gives comparable results with the experimental data, to apply this model rheological classification of the fluid model and rheological constants should be known. The model is restricted to Bingham Plastic and Power-Law fluids.

Clapp [8] obtained an integrated mean linear velocity, V, from the velocity profile in a turbulent core and obtained a relationship between friction factor and Reynolds Number:

$$\sqrt{\frac{1}{f}} = \frac{2.69}{n} - 2.95 + \frac{4.53}{n}\log\left[N_{\mathrm{Re},Cl}\left(f\right)^{1-n/2}\right] + 0.68\left(\frac{5n-8}{n}\right) \quad \text{.....(44)}$$

where,

$$N_{\mathrm{Re},Cl} = \frac{D^n V^{2-n}\rho}{K8^{n-1}} \quad \text{.....(45)}$$

Nikuradse [9] introduced the effect of roughness and separated the curves for each level of tube roughness for turbulent flow of Newtonian fluids. He observed that, in the fully turbulent region, friction factors are dependent on roughness but independent of Reynolds number. Experimental studies show that:

$$\sqrt{\frac{1}{f}} = 4\log\frac{R}{e} + 3.48 \quad \text{.....(46)}$$

Colebrook [10] recommends an empirical relationship for the transition region before fully developed turbulent flow of Newtonian fluids occurs, so that the friction factor is dependent on both roughness and Reynolds number;

$$\sqrt{\frac{1}{f}} = 4\log\frac{R}{e} + 3.48 - 4\log\left[1 + 9.35\frac{R/e}{N_{\mathrm{Re}}\sqrt{f}}\right] \quad \text{.....(47)}$$

API equations [11] use effective viscosity while defining the regime of flow by using the Reynolds number. The Reynolds number for pipe flow can be calculated as follows:

$$N_{\mathrm{Re},P} = \frac{V_p D \rho}{\mu_{eff,P}} \quad \text{.....(48)}$$

The friction factors for laminar and turbulent flow can be calculated as:

$$f_{P,lam} = \frac{16}{N_{\mathrm{Re},P}} \quad \text{.....(49)}$$

$$f_{P,tur} = \frac{a}{\left(N_{\mathrm{Re},P}\right)^b} \quad \text{.....(50)}$$

where

$$a = \left(\log n + 3.93\right)/50 \quad \text{.....(51)}$$

$$b = \left(1.75 - \log n\right)/7 \quad \text{.....(52)}$$

The frictional pressure loss gradient is calculated from Fanning equation (in field units) as:

$$\frac{\Delta P}{L_m} = \frac{f_p V_p^{\,2} \rho}{25.81 D} \quad \text{.....(53)}$$

<u>Turbulent Flow Of Non-Newtonian Fluids in Annuli:</u>

Although a large amount of experimental work has been done in circular pipes, there is a lack of experimental data for turbulent flow of non-Newtonian fluids through annular spaces. For this reason, while studying turbulent flow in annuli it was assumed that the relation between the Reynolds number and friction factor for pipe flow applies

equally well to the other geometries. Thus, the only modification needed in the Fanning equation is to change the diameter to a more appropriate form.

Fredrickson and Bird [12] used conventional Newtonian *f* vs. Reynolds number charts that were derived for turbulent flow in smooth pipes. Consequently:

$$f = \frac{\Delta P g_c R_2 \left(1 - \bar{K}^2\right)}{L\left(1 + \bar{K}\right)\rho V^2} \quad \text{.....(54)}$$

Wilcox [13] suggested that knowing the radial position in the annulus at which the linear velocity is maximum could be used to determine an expression between friction factor and Reynolds number, but there is no method available for its prediction under non-Newtonian turbulent conditions.

API equations [11] for annular flow treat the annulus as a hydraulic diameter (OD-ID) and assumes smooth pipes, so the Reynolds number for annular flow change as follows:

$$N_{\mathrm{Re},P} = \frac{928 V_a \left(D_2 - D_1\right)\rho}{\mu_{ea}} \quad \text{.....(55)}$$

The friction factors can be calculated from the following equations as:

$$f_{a,lam} = \frac{24}{N_{\mathrm{Re},ann}} \quad \text{.....(56)}$$

$$f_{a,tur} = \frac{a}{\left(N_{\mathrm{Re}.an}\right)^b} \quad \text{.....(57)}$$

where

$$a = \left(\log n + 3.93\right)/50 \quad \text{.....(58)}$$

$$b = \left(1.75 - \log n\right)/7 \quad \text{.....(59)}$$

a and b obtained from experimental data. Frictional pressure loss is calculated by substituting the appropriate friction factor into the Fanning equation for the annulus and obtaining the friction loss pressure gradient as:

$$P_a / L_m = \frac{f_a V_a{}^2 \rho}{25.81(D2 - D1)} \quad \text{.....(60)}$$

Pilehvari [14] developed the concept of equivalent diameter and introduced the term ‘effective diameter’ which accounts for both the annular geometry and effects of a non-Newtonian fluid; thus it links Newtonian pipe flow and non-Newtonian annular flow. He proposed that the effective diameter for non-Newtonian pipe flow is equal to the diameter of a circular pipe that would have the identical pressure drop for flow of a Newtonian fluid when the viscosity is equal to the apparent viscosity and using the same average velocity as with non-Newtonian flow. Effective diameter can be shown as follows;

$$D_{eff} = 4ND/(3N+1) \quad \text{.....(61)}$$

He extended the effective diameter definition to concentric annuli by including the effect of geometry as well. He defined effective diameter for non-Newtonian flow through a concentric annulus as the diameter of a circular pipe that would have identical pressure drop for flow of a Newtonian fluid with viscosity equal to the effective viscosity, and has a velocity equal to the non-Newtonian annular flow velocity. The effective viscosity is based on the average wall shear rate in the annulus.

RHEOLOGICAL CHARACTERIZATION OF DRILLING FLUIDS UNDER HIGH PRESSURE AND HIGH TEMPERATURE:

Rheological models provide assistance in characterizing fluid flow. While determining the flow regime by using the Reynolds number and predicting friction coefficients and parasitic pressure losses, rheological parameters such as viscosity, consistency index, density, yield stress control the fluid system and flow under consideration. All these parameters are subject to change under high pressure and high temperature conditions. For this reason, it is important to determine the response of the rheological model to wellbore conditions to fully understand the fluid performance and obtain accurate parasitic pressure loss results. Several investigators have attempted to model the effect of temperature and pressure on drilling fluid rheology through the shear rate history of the fluid.

Garvin and Moore (1970) [15] used a pipe rheometer to determine fluid properties from lower laminar flow to fully turbulent flow with temperatures up to 350 ^{0}F. Water-based drilling fluids were used as the testing fluid and concluded that the Bingham Plastic model gave a reasonable fit with the model in laminar flow, but data started to diverge under transition flow. They also concluded that plastic viscosity decreases with increasing temperature, yield point may increase or decrease with increasing temperature depending upon the solid content of the fluid, power-law index (n) decreases with increasing temperature, and consistency index (K) increases with increasing temperature.

Methven and Baumann (1972) [16] analyzed the performance of oil based muds and invert emulsions at high temperatures. They uses PVT data, computed downhole transient temperatures and Bottom-Hole Conditions (BHC) rheometer to determine

rheological characteristics of the fluids. They concluded that density of oils varies inversely with temperature and directly with pressure, which is also a function of the relative density of the oil. Moreover, it was concluded oil based muds that contain asphalts were more stable under high temperatures.

McMordie, Bennett and Bland (1975) [17] used a BHC viscometer to determine the viscosity of the oil based muds at temperature up to 650 ^{0}F and pressure up to 20000 psig. They reported, the best model to describe the viscosity of oil based muds at constant temperature and pressure is the Power–Law model. Analysis showed that shear stress is directly proportional to pressure and inversely proportional to temperature. They modified the Power-Law model to depict these effects as,

$$\ln \tau = \ln K' + n \ln \gamma + AP + B/T \quad \text{.....(62)}$$

The constants A and B must be determined experimentally.

McMordie, Bland and Hauser (1982) [18] investigated the change in density of water based and oil based drilling fluids in the pressure interval of 0-14000 psig and temperature interval of 70-400 ^{o}F under laboratory conditions. They concluded that the change in density of the drilling fluid is independent of its initial density; and oil based drilling fluids become denser at high pressure and temperature due to greater compressibility compared to water-base drilling fluids. Density at a given pressure and temperature was computed as:

$$\rho_1 = \rho_0 e^{0.000319N} - 1.064 * 10^{-5} P^{1.063} \quad \text{.....(63)}$$

De Wolfe, Coffin and Byrd (1983) [19] studied the rheological changes of less toxic oil drilling fluids under pressure and temperature. They propose a general procedure for compiling a base of base-oil, laboratory prepared oil-base drilling fluids and oil-base

drilling fluids used in the field. An HPHT rotational viscometer capable of temperature in the range of ambient to 500 ^{o}F and pressure in the range of 0-12000 psig , was used to investigate the rheological properties. Their research showed that, less toxic oils become more viscous as pressure is increased, but the viscosity differences among the oils tends to decrease with increasing temperature even if the pressure is increased. Moreover, temperature has the greatest effect on viscosity reduction below 200 ^{o}F.

Houwen and Geehan (1986) [20] compared rheological models for invert emulsion drilling fluids under pressures up to 1000 bar and temperatures up to 140 ^{o}C. They found that Herschel-Bulkley and Casson equations fit well with the experimental rheograms, but Casson's model is more reliable in terms of extrapolation purposes so that it is chosen as the rheological model. Then, they developed exponential expressions to model temperature and pressure behavior of the Casson model. Their modified model is based on relations derived by Eyring for pure liquids and showed how changes in viscosity or yield point with change in pressure can be related to temperature or vice versa. As a result, they obtained viscosity and yield stress values as functions of pressure and temperature. The generalized form of these equations can be shown as,

$$\overline{VIS}(P,T) = A\exp\left(\frac{E}{RT} + \frac{YV_a P}{RT}\right) \quad \text{.....(64)}$$

API Recommended Equations [11] show the effect of temperature and pressure on viscosity as follows:

$$\mu_e(T_2) = \mu_e(T_1)\exp\left[\beta\left(\frac{T_2 - T_1}{T_1 T_2}\right)\right] \quad \text{.....(65)}$$

and

$$\mu_e(P_2) = \mu_e(P_1)\exp\left[\alpha(P_2 - P_1)\right] \quad \text{.....(66)}$$

Equation (65) is valid until a thermal decomposition or transition of any component in the drilling fluid take place. At this point drilling fluids do not follow any mathematical model. Equation (66) can be neglected for water based drilling fluids since they are only slightly compressible. On the other hand, pressure has a great effect on oil based drilling fluids and invert emulsions.

EXPERIMENTAL FACILITY

The Advanced Cutting Transport Facility loop located on the North Campus of The University Of Tulsa can function as a pipe viscometer. The loop consists of three rheology sections with nominal diameters of 2”, 3” and 4”. In addition to these, a drilling section is available to study the annular flow. The drilling section consists of a 6” external pipe and an inner 3.5” drillpipe. The drillpipe will be installed after the piping system constants and calibrations for the 6” section have been completed. All of the pipes are made of steel that tested to 3300 psig for not less than 30 minutes and not more than 60 minutes. The test sections are 65 ft in length. Five feet of pipe at both the entrance and exit are available for use as a quieting section between the pressure taps and the entrance or exit to the test section. Thus, a separation of 55 ft between pressure taps is available for measuring pressure drop values.

A Halliburton Model HT 400 triplex fracturing pump is currently used to circulate mud in the system. Its maximum operating pressure is 11,200 psia and it can give flowrates as high as 250 gpm when the system pressure is 1000 psia. Due to the nature of this piston-type pump, pulsation occurs on each stroke while it is pumping fluid. Since the data acquisition system is sensitive, this pulsation generates wavy data recordings. To

counteract the pulsation effect, a pulsation dampener was installed at the discharge end of the pump and it was observed that the pulsation effect no longer exists.

As seen in Figure 1, the test sections are connected in series so that the same flowrate is passing through all the test sections (2”, 3”, 4” and annular section). This may help to see the effect of diameter on the flow regime and to control the flowrate in all testing sections. However by adjusting the valves properly, parallel flow through 2” and 3” test sections can also be achieved. Moreover, again by adjusting valves, annular flow alone can be studied at various flow rates.

To measure the differential pressure loss through the sections, a Rosemount Model 3051CD Differential Pressure Transmitters were installed. They measure the differential pressures in the range of 0.5 inH_2O to 250 inH_2O with 0.075% accuracy. Static pressure in the system is measured by two ways. Liquid-filled Bourdon Tube Pressure Gauges, that range between 0 and 2000 psig in 20 psig increments, measure pressure on the system (while adjusting the back pressure with a choke). Moreover, these gauges are used to check whether data acquisition system is working properly or not by comparing the readings of the computer with the gauges. One of these gauges was installed just after the pump exit to the discharge line to see the system pressure. Another Bourden gauge was installed before the choke to observe and control the back pressure applied to the system and a third gauge was installed to the downstream part of the choke to see if choke is working properly. Static pressure distribution in the system is also determined by using Rosemount Model 3051CA Absolute Pressure Transmitters which measure absolute pressures from 0.167 to 4000 psia with 0.05% accuracy. These

transmitters were mounted to the middle of each test section and to the discharge line just after the pump exit.

Choke valves are used to control and fix the system pressure. Pressure in the system is increased by decreasing the flow area. This is accomplished by injecting N_2 to the seals that are present in the choke as flow restrictive elements.

Doppler Sonic flowmeters, capable of measuring flowrates in the range of 0 to 450 gpm, are used to measure the volumetric flowrate in the system. Two Doppler Sonic flowmeters were mounted to the 4'' drilling fluid discharge line, 5 ft apart from each other to check if both are working properly.

Differential pressure transducers, absolute pressure transmitters and Doppler flowmeters were connected to a computer located in the control room near the loop. The system pressures, differential pressures and flowrates can be measured, data can be stored and averaging intervals can be controlled using the data acquisition system. The data acquisition system utilizes LABView™ software which is very powerful for data storage and logging, real time display and on-line analysis.

EXPERIMENTAL TEST PROCEDURE:

Advanced Cutting Transport Facility (ACTF) Loop (Table-1):

First, drilling fluid rheological properties are measured using Model 3500 Fann rotational viscometer at low and high shear rates. From this data, a rheological model of the fluid under ambient conditions is determined.

Then, the Halliburton triplex piston pump is used to circulate drilling fluid through the system. It is desirable to circulate the fluid at high flowrates to make sure that the 6” pipe is full.

After all the air is removed from the system, the flowrate is adjusted to 300 gpm without any back pressure. Differential pressures from each test section, static pressures from the middle of each pipe and at the pump exit, and flowrate are recorded after stabilization and each time the flowrate is decreased by 50 gpm intervals.

When 50 gpm flowrate data were recorded, system is again brought up to 300 gpm and back pressure of 200 psig is applied to the system by injecting N_2. Data is taken after stabilization of the flow is established. Then, the flowrate is again decreased by 50 gpm intervals and after each reduction of the flowrate, back pressure of the system is kept constant at 200 psig by adjusting the choke.

After all the flowrate ranges for a given back pressure are analyzed, the flowrate is readjusted to 300 gpm and the back pressure specified for a particular test is increased by 200 psig.

Once high temperature capability is added to the system, the above procedure will be carried at intervals of 25 ^{o}F starting from ambient temperature of the fluids and ending with the maximum temperature that the heat exchanger can convey to the fluid (220 ^{o}F planned initially).

RESULTS AND DISCUSSION:

Experiments with water without Back Pressure:

Preliminary Tests with water using Piston-Type Pump:

The first experiments with the ACTF were carried out to calibrate the devices and to check the repeatability of data recorded by the differential pressure transducers, absolute pressure transducers and flowmeters. It was decided to use water as a testing fluid for calibration process. It was planned to install one of the flowmeters to the 4" discharge line right after the exit of the pump to see the total flow circulating in the system and to install the other flowmeter to the 3" test section. The flowrate in the 2" test section should be the difference between these two flowmeter readings.

In calibration tests 2" and 3" pipes were connected parallel to give the same pressure drop along the same differential length. Results of these experiments are shown in Table-2. According to the flowmeter readings most of the flow was passing through the 3" test section, but flow through the 2" test section does not show an increasing trend with increasing total flowrate of the system. Comparison of the experimental data with the results from published models [21] (Figures 2-4) show that the differential pressure transducers are overestimating the pressure losses and there is no direct relation between the flowrate and pressure losses. Comparison of experimental pressure loss in the 2" and 3" test sections (Figure 5) show that there is no agreement in the readings of these devices either. Inaccuracy of the data may be due to errors in the calibration of the devices or due to accuracy of the devices. It is also possible that, since all the differential pressure transducers and static pressure transmitters were mounted on top of the pipes through large diameter connection parts (weld-o-lets), additional turbulence may have

been generated in the area where data was recorded. A close look at the experimental data suggested that, the piston displacement nature of the pump could also be affecting the data.

Preliminary Tests with water using Centrifugal Pump (W/O Back Pressure):

A centrifugal pump was used to diminish the effects of piston impact. In addition use of centrifugal pump makes it possible to check the accuracy of the flowmeters since flowrate in this type of pump is set to a desired rate by using a Fisher control valve and measured by using a mass flowmeter. To decrease turbulence, differential pressure transmitters and static pressure transducers were mounted to the middle of the pipes using small taps instead of large diameter connection parts (weld-o-lets). Six sets of data from four experiments were collected using the centrifugal pump to check the repeatability of the results and how they were compared with theoretical calculations. Results for each test section are shown in Table-3.

It can be seen that sonic doppler flowmeter readings are generally underestimating the actual flowrate. In some cases, the flowmeter in the 3” test section was recording higher flowrates than the flowmeter in the discharge line. It was concluded that, this might be due to the nature of the Doppler flowmeter. Since water used in the test did not contain that much solid particle in it, this may have caused the discrepancy of sonic doppler flowmeters readings. However, the results show good repeatibility and match the theoretical data within the accuracy range of the pressure devices (Figures 6-7). A small over-reading of experimental pressure losses is acceptable, because the theoretical calculations assumed smooth pipe. As seen in Figure (7) that differential

pressure losses in the 2” and 3” pipes were almost the same. Repeatability in recordings decrease as flowrate increases because at higher flowrates the error range of the differential pressure transmitter increases (ie.±6 inH_2O at 300 gpm). From this point of view, it may be concluded that data recordings are repeatable.

Determination Of Roughness Of 6” Pipe By Using Centrifugal Pump Experimental Data:

Since the flowmeters were not recording reliable values, the only reliable flowmeter data is given by the mass flowmeter. For that reason, comparison of actual flowrates and theoretical flowrates was done only for the 6” pipe where total flow is passing through. The friction factor vs. Reynolds number plot is given in Figure 8. The relative roughness of the 6” pipe was determined to be approximately 0.00060 (Table-4). It can be seen that there are still some problems of low flowrate readings which might be due to the inability to achieve flow stabilization. To check the validity of the roughness estimation in the 6” pipe, actual pressure losses were compared with theoretical calculations using the 0.00060 as the relative roughness of the pipe (Figure 9). Comparability of experimental and theoretical results were excellent.

Preliminary Tests with water using Piston-Type Pump with Pulsation Dampener:

Since the piston type pump produced fluctuations in the data, a pulsation dampener was installed on the system to reduce the effect of strokes. To help control the flowrate, an rpm counter was installed on the pump.

Experiments using the dampener agree with the experiments using the centrifugal pump (Table 5). It was also observed in the experiments using the triplex pump that sonic

doppler flowmeters were not working properly. The flowmeter in the discharge line is underestimating the actual flowrate. The flowmeter in the 3” test section gave sporadic results in all ranges of flowrate. After it is determined that the differential pressure transducers and absolute pressure transmitters are working properly, the second phase will begin.

FUTURE WORK:

The first phase of the project is in progress. Currently addition of a mass flowmeter to the flow loop is under progress. After installation of the mass flowmeter, we plan to conduct more experiments to define the roughnesses of 2”, 3” and 4” test sections and check the system under pressure by using water as a testing fluid.

In the second phase, we will add heating capability to the system. At the same time, experiments with synthetic based fluids that will be provided by Petrobras will be started. The Petrobras mud is essentially a synthetic system (invert emulsion) formed by hydrogenerated isoparaphine, emulsifiers, brine, CaO, and organophylic clay. The rheological data of the mud system obtained by using rotational viscometer is given in Table-6.

We will study the effect of pressure on the synthetic fluid as the first step of the experimental analysis. Simultaneously, rheological characterization of the drilling fluid under high pressure and high temperature will be carried by using the HPHT Rheometer. Next, the effect of temperature on the fluid will be studied using the ACTF pipe viscometer and rheological data obtained from the pipe viscometer and the rotational viscometer will be compared.

Empirical and semi-empirical solutions derived for turbulent flow by previous investigators will be compared to the experimental results. Based on these experimental results, modifications of the existing models will be attempted. In addition, we plan to study the effect of drag reducers on turbulent flow of the synthetic based drilling fluids.

Finally, a computational tool will be developed to predict the bottom hole pressure and equivalent circulating density for a given drilling fluid system and a geometry.

CONCLUDING REMARKS

- Most of the turbulent flow models for non-Newtonian fluids is generally derived with the assumption that the fluids that are non-Newtonian in laminar flow, behaves Newtonian in turbulent flow. Previous investigators defined this Newtonian behavior by introducing different viscosity definitions to flow equations that were derived for laminar flow.
- Most of the experimental work done on turbulent flow have been based on small scale apparati with diameters ranging between 1/8”-1’ and lengths ranging between 1’-10’. However, such sizes do not reflect the field conditions and may produce unrealistic results for turbulent flow in pipes and annuli.
- Turbulent flow in annuli is not well defined yet and very few experimental data is available. This study may help to understand the mechanism of turbulent flow of non-Newtonian fluids in annular geometries.
- Most attempts to characterize the rheology of emulsions have used rotational viscometers. However, rheological model predictions from rotational viscometer

reflects fluid behavior under laminar flow conditions. Therefore, it would be beneficial to study the rheological properties of drilling fluids in a pipe viscometer to examine the effect of cyclical variations in temperature and pressure and turbulence effects. Data obtained from pipe a viscometer and rotational viscometer will be compared for possible correlation among them. Such a comparison will be both very interesting and very informative.

- Although synthetic drilling fluids have advantages over water-base drilling fluids in terms of operational features (lubrication, shale inhibiton, prevention of gas hydrates in deepwater offshore drilling), and advantages over conventional oil base drilling fluids in terms of environmental constraints, they are very sensitive to pressure and temperature changes. This may cause rheological instability problems in the well and make calculation of pressure losses difficult.
- Determination of rheological models of synthetic drilling fluids flowing in turbulent flow under high pressure and temperature will allow the prediction of pressure losses and equivalent circulating densities in the wellbore without using expensive tools like pressure while drilling (PWD) and measurement while drilling (MWD)
- We will attempt to find the best rheological model for a given mud system under high pressure and temperature and at both low and high shear rates. This type of rheological model would be very useful in the development of models simulating turbulent and laminar flow of synthetic based drilling fluids in pipes and annuli.

NOMENCLATURE

A	pressure constant
A’	constant in Arrhenius equation
A_n	a function of n, constant at constant n, dimensionless
a	friction factor constant
A_{1n}	$1.628A_n$, dimensionless
B	temperature constant
B_n	a dimensionless function of n
b	friction factor exponent
c	$\tau_y/\tau_w=r_p/R$
D	tube diameter, ft
D_1	inner annulus diameter, ft
D_2	outer annulus diameter, ft
E	least squares sum
e	height of roughness projections inside tube, ft
f	Fanning friction factor, dimensionless
g_c	conversion factor, 32.174 lbmassft/lbforcesec^2
K	fluid consistency index, lbmasssec^{n-2}ft^{-1}
K’	consistency index at the wall, lbforcesec$^{n'}$ft^{-2}
K	R_1/R_2
L_m	measured depth, ft
n	flow behavior index, dimensionless
N	generalized flow behavior index of Metzner and Reed
N^0_{Re}	$D^nV^{2-n}\rho/K$
ΔP	pressure drop, upstream minus downstream conditions, lbforce/ft^2
P	pressure, psig
P_a	pressure drop in annulus
P_n	a dimensionless function of n
R	tube radius, ft
R_1 and R_2	inner and outer radii of annulus, ft

u	local linear velocity in the x-direction at *r* or *y*, ft/sec
u^*	friction or shear velocity, ft/sec
u_m	maximum linear velocity (at tube centerline), ft/sec
V	mean linear velocity in the *x*-direction, ft/sec
V_a	average bulk velocity in annulus, ft/sec
Y	1, if VIS stands for plastic viscosity or Casson high shear viscosity
Y	Y_B or Y_C if VIS stands for YP or τ_Y
y	normal distance from tube wall R-r, ft
α	pressure constant
β	temperature constant
η	plastic viscosity, lbmass/ftsec
μ, μ_{eff}, μ_{ea}	viscosity, effective viscosity, effective viscosity in annulus lbmass/ftsec
ξ	y/R, dimensionless
ρ	density, lbmass/ft^3
ρ_0	density at 70 ^{o}F, 0 psig, lb/gal
ρ_1	density at T, P, lb/gal
γ	shear rate, sec^{-1}
τ_{rx}	shear stress in *x*-direction on surface normal to *r*, lbforce/ft^2
τ_w	shear stress at the wall of a tube, DΔP/4L, lbforce/ft^2
τ_y	yield stress, lbforce/ft^2

REFERENCES

1. Caldwell, D.H., and Babbitt, H.E., Trans. A.I.Ch.E., 25, 237, 1941.

2. Skelland, A.H.P.: " Non-Newtonian Flow and Heat transfer", John Wiley and Sons, Inc., New York,NY, 1967.

3. Weltmann, Miss R.N., Ind. Eng. Chem., 48, 386-7, 1956.

4. Alves, G.E., Boucher, D.F., and Pigford, R.L., Chem. Eng. Prog., 48, 385-393, 1952.

5. Metzner, A.B., and Reed, J.C., A.I.Ch.E.J., 1, 434, 1955.

6. Dodge, D.W., and Metzner, A.B., (a) A.I.Ch.E.J., 5, 189-204, 1959, (b) A.I.Ch.E.J., 8, 143, 1962.

7. Tomita, Y.: Bull. Of J.S.M.E. (Japan Soc. Mech. Eng.), 2, 10-16, 1959.

8. Clapp, R.M., International Developments in Heat Transfer, Part III, 652-661; D-159; D-211-5, ASME, New York, 1961.

9. Nikuradse, J., Forschungsh. Ver. Dtsch. Ing., p. 356, 1932.

10. Colebrook, C.F., J. Inst. Civil Engrs., London, 11, 133, 1938-1939.

11. Recommended Practice On The Rheology and Hydraulics of Oil-Well Drilling Fluids, Exploration and Production Department, API Recommended Practice 13D, Third Edition, June 1, 1995.

12. Fredrickson, A.G., and Bird, R.B., Ind. Eng., Chem, 50, 1599, 1958.

13. Wilcox, W.R., Ind. Eng. Chem., 50, 1600, 1958.

14. Pilehvari, A.A. and Reed, T.D.: "A New Model for Laminar, Transitional, and Turbulent, Flow of Drilling Muds", SPE 25456, SPE?IADC Drilling Conference, Amsterdam, February 22-25, 1993.

15. Garvin, T.R., Moore, P.L.: “A Rheometer for Evaluating Drilling Fluids at Elevated Temperatures”, SPE 3062, paper presented at the 45th Annual Meeting of SPE, Houston, TX, October 4-7, 1970.

16. Methven, N.E. and Baumann, R.: "Performance of Oil Muds At High Temperatures", SPE 3743, paper presented at the SPE-European Spring Meeting, Amsterdam, May 16-18, 1972.

17. Mc Mordie Jr., et. al.: “The Effect of Temperature and Pressure on the Viscosity of Oil Based Muds; JPT 4974, July 1975, 883.

18. Mc Mordie Jr., et. al. “ The Effect of Temperature and Pressure on the Density of Oil-Base Muds”, SPE 11114, paper presented at the 57th Annual Technical Conference of SPE, New Orleans, LA, September 26-29, 1982.

19. De Wolfe, R.C., et. al.: “Effects of Temperature and Pressure on the Rheology of Less Toxic Oil Muds”, SPE 11892, paper presented at the Offshore Europe Conference, Aberdeen, September 6-9, 1983.

20. Houwen O.H. and Geehan, T.: “Rheology of Oil-Base Muds”, SPE 15416, paper presented at the 61st Annual Technical Conference of SPE, New Orleans, LA, October 5-8, 1986.

21. Bourgoyne, A.T., Jr., Chenevert, M.E., Milheim, K.K. and Young, F.S., Jr.: APPLIED DRILLING ENGINEERING, SPE Textbook Series, 1986, 176-182

TABLE 1- Synthetic Based Drilling Fluid Experimental Test Matrix (Pipe Viscometer)

Fluid Temperature, ^{0} F	Back Pressure, psi	Flowrate, gpm
75	0-1400 (200 psi increments)	50-300(50 gpm increments)
100	0-1400 (200 psi increments)	50-300(50 gpm increments)
125	0-1400 (200 psi increments)	50-300(50 gpm increments)
150	0-1400 (200 psi increments)	50-300(50 gpm increments)
175	0-1400 (200 psi increments)	50-300(50 gpm increments)
200	0-1400 (200 psi increments)	50-300(50 gpm increments)

TABLE-2 Water Experimental Data Analysis Results (Piston Type Pump)

Total Q	Q(3" pipe)	Q(2" pipe)	DP @ 2"	DP @ 3"	DP @ 6"	DP @2" (Theo.)	DP @3" (Theo.)	DP @6 (Theo.)
GPM	GPM	GPM	inH2O	inH2O	inH2O	inH2O	inH2O	inH2O
67.1393617	60.870426	6.2689362	9.172979	31.51234	2.783191	0.977797739	7.328435324	0.33383807
146.9992857	129.72821	17.271071	28.05143	67.20607	4.618214	5.760610814	27.54929175	1.31561069
149.0016346	128.35481	20.646827	25.48625	68.5976	4.619038	7.873232924	27.04091692	1.34713170
166.7226829	146.00195	20.720732	32.47146	64.1239	4.214634	7.922617664	33.87878471	1.63989657
172.5686364	150.42909	22.139545	34.95182	62.86409	5.014545	8.896209876	35.69693039	1.74184304
186.0906452	157.98032	28.110323	37.02452	60.02871	4.416452	13.5106112	38.8915643	1.98766732
187.8828205	165.44462	22.438205	45.95462	55.09872	6.097179	9.107286401	42.16404644	2.02128766
194.9553846	165.11385	29.841538	44.58923	51.39846	5.627692	15.00019521	42.01663642	2.15631603
196.376	162.279	34.097	45.305	54.796	5.814	18.94144431	40.76235183	2.18388853
246.9615385	223.72385	23.237692	62.59615	35.43846	5.506154	9.682723701	71.49845426	3.26157270
250.5121739	229.61261	20.899565	72.03935	45.34	9.218043	8.042665097	74.82430654	3.34407657
258.33	226.8	31.53	72.16579	50.39789	9.706316	16.5168317	73.22771896	3.52883805
268.2892593	243.58926	24.7	79.27556	35.11111	9.007778	10.77406182	82.97588707	3.77034856
271.0660606	244.82909	26.23697	84.31091	77.63424	6.89	11.97453682	83.71638242	3.83890401
273.6404762	247.43143	26.209048	76.83333	61.97524	7.231429	11.95224439	85.2798009	3.90293520
276.6186441	250.53932	26.079322	84.58678	79.69373	7.519492	11.84890766	87.16316458	3.97757415
293.2955172	267.33414	25.961379	94.45828	74.59034	6.725172	11.75529086	97.64396455	4.4066671

Table-4 Roughness Analysis of 6" Pipe

Flowrate GPM	Abs. Rough., E in	Rel. Rough, E/d
50	-0.013553488	-0.002352628
100	0.001817511	0.000315485
150	0.00352535	0.000611934
200	0.003589628	0.000623091
250	0.003399828	0.000590145
300	0.003116531	0.000540971

Table-5 Water Experimental Data Analysis Results (Triplex Pump with Dampener)

Flowrate GPM	Q (3" pipe) GPM	Q (2" pipe) GPM	Q (6" pipe) GPM	DP @ 2" inH2O	DP @ 3" inH2O	DP @ 6" inH2O
50	227.8770479	-183.0277846	44.84926325	4.134272137	3.720254129	0.13753692
100	259.1158916	-186.6807527	72.43513891	16.19204595	14.71232278	0.72949314
150	171.8874283	8.938314839	180.8257431	35.8049066	32.69848447	1.64649995
200	174.6955907	9.984971306	184.680562	60.78540043	55.67476526	2.84196003
250	219.4061444	7.419451655	226.825596	90.131839	82.62144274	4.26553650
300	262.9024834	6.086436321	268.9889197	124.9854517	115.2680097	6.02580277
50	412.7174763	-368.4439641	44.2735122	4.155672202	3.735917394	0.14809794
100	169.5164557	-99.08559418	70.43086154	16.42088888	14.94622334	0.77178530
150	131.0216367	6.410051205	137.4316879	36.09075902	33.0270692	1.72096315
200	173.5973845	9.523236394	183.1206209	59.94985952	55.02959987	2.8918032
250	217.4440913	8.311436938	225.7555283	90.43710949	83.38272055	4.40563277
300	260.1329578	7.371288713	267.5042465	126.8620937	117.2552275	6.14571160
50	450.6860033	-405.8683366	44.81766667	3.905708533	3.4725217	0.13283964
100	230.11685	-154.4750075	75.6418425	15.57633598	14.19373665	0.74854655
150	123.8044675	12.1484325	135.9529	34.86318508	31.9327296	1.70283402
200	167.8762725	11.9156275	179.7919	58.82705755	54.0814125	2.88434889
250	211.27049	11.61836	222.88885	89.59436675	82.65652578	4.38659969
300	251.91883	14.19397	266.1128	125.55974	116.037155	6.0856889

Table-6 Rotational Viscometer Readings Of Petrobras Synthetic Mud System

Density	8.6 lbm/gal	
FANN READINGS	600 rpm	65
	300 rpm	40
	200 rpm	31
	100 rpm	21
	6 rpm	9
	3 rpm	8

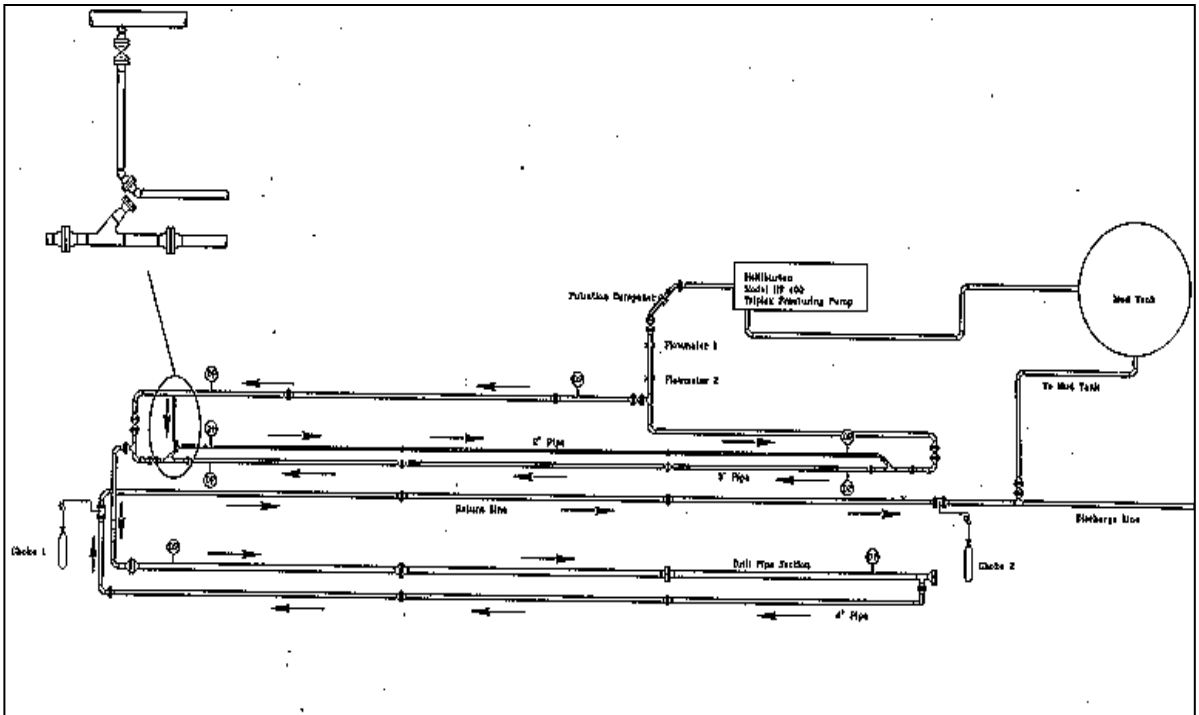

Figure 1: Schematic Representation of Advanced cutting Transport Loop (ACTF) Piping System

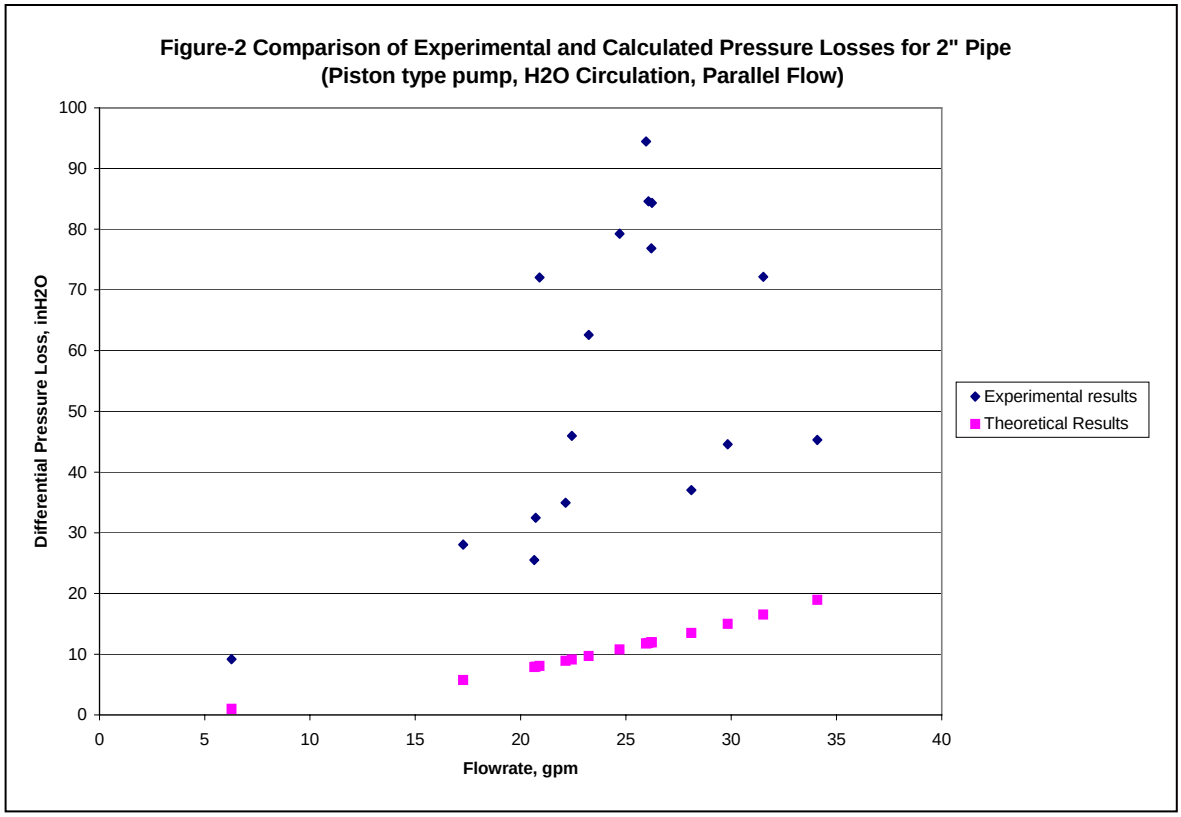

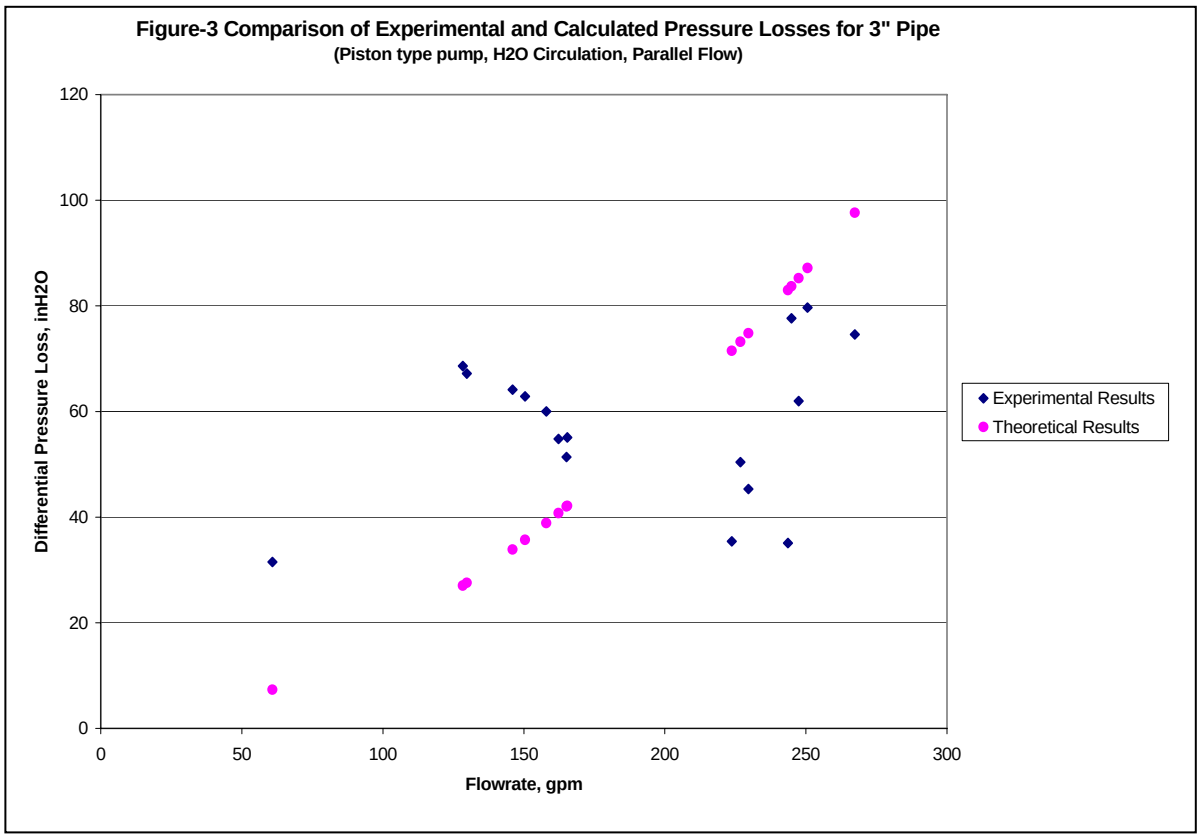
Figure-3 Comparison of Experimental and Calculated Pressure Losses for 3" Pipe
(Piston type pump, H2O Circulation, Parallel Flow)
Differential Pressure Loss, inH2O
Flowrate, gpm
0
20
40
60
80
100
120
0
50
100
150
200
250
300
Experimental Results
Theoretical Results

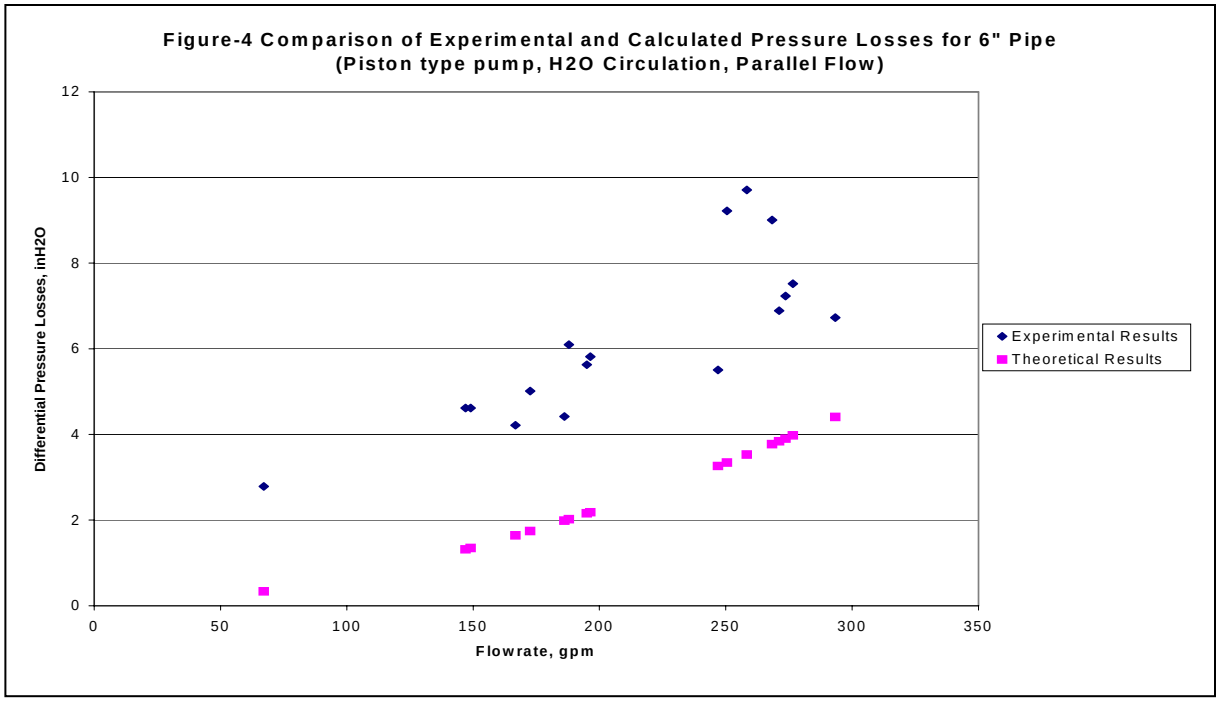
Figure-4 Comparison of Experimental and Calculated Pressure Losses for 6" Pipe
(Piston type pump, H2O Circulation, Parallel Flow)
Differential Pressure Losses, inH2O
Flowrate, gpm
0
2
4
6
8
10
12
0
50
100
150
200
250
300
350
Experimental Results
Theoretical Results

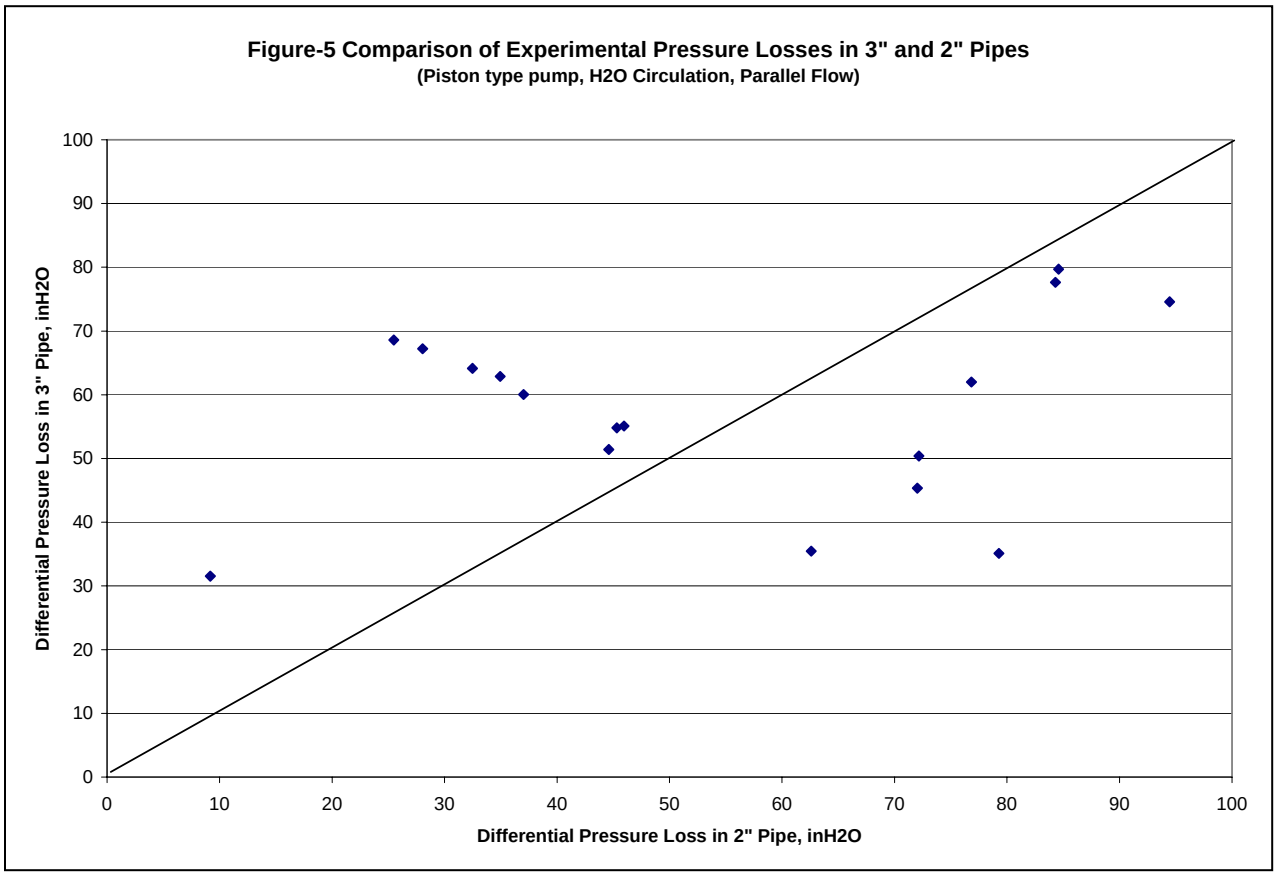
Figure-5 Comparison of Experimental Pressure Losses in 3" and 2" Pipes
(Piston type pump, H2O Circulation, Parallel Flow)
Differential Pressure Loss in 3" Pipe, inH2O
Differential Pressure Loss in 2" Pipe, inH2O
0
10
20
30
40
50
60
70
80
90
100

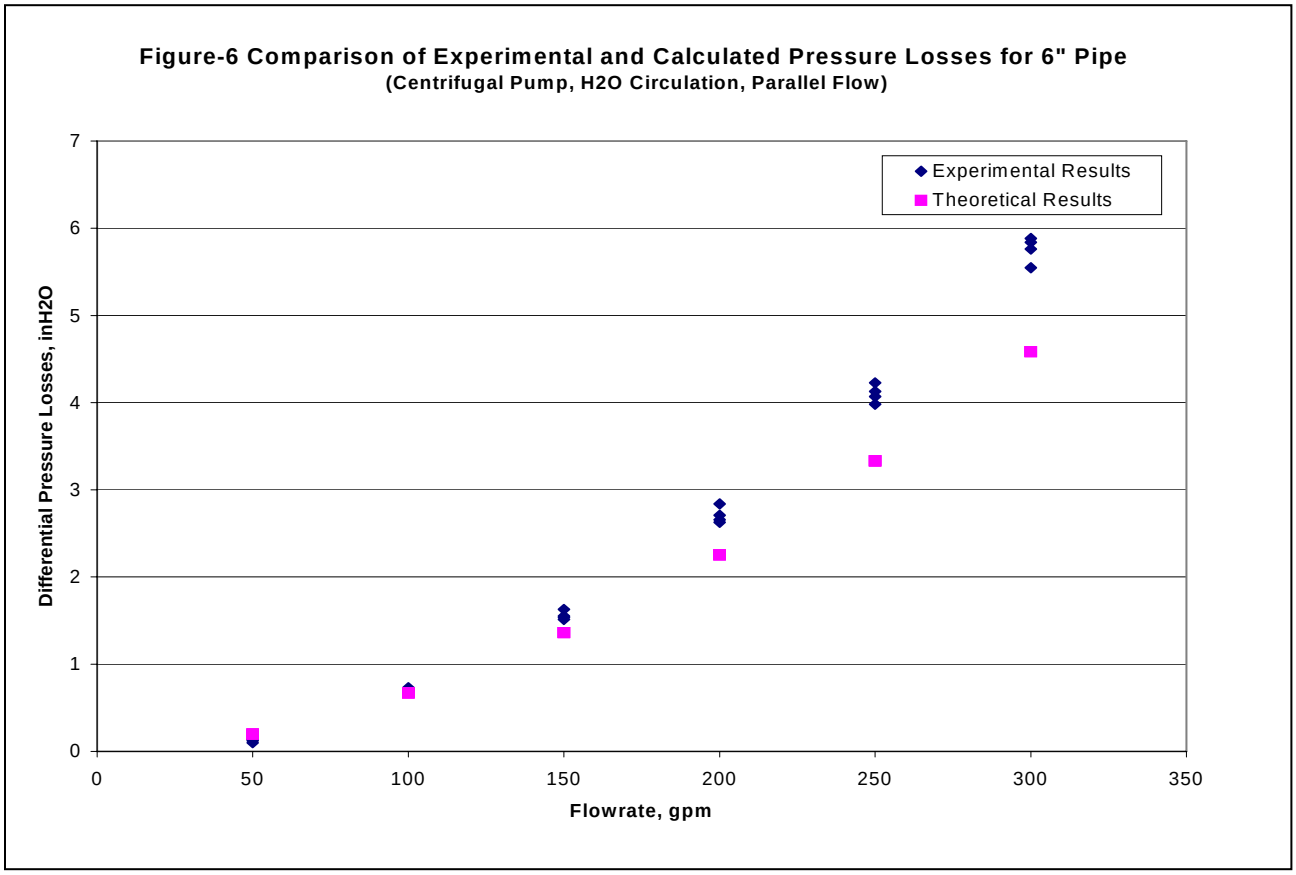
Figure-6 Comparison of Experimental and Calculated Pressure Losses for 6" Pipe
(Centrifugal Pump, H2O Circulation, Parallel Flow)
Experimental Results
Theoretical Results
Differential Pressure Losses, inH2O
Flowrate, gpm
0
1
2
3
4
5
6
7
0
50
100
150
200
250
300
350

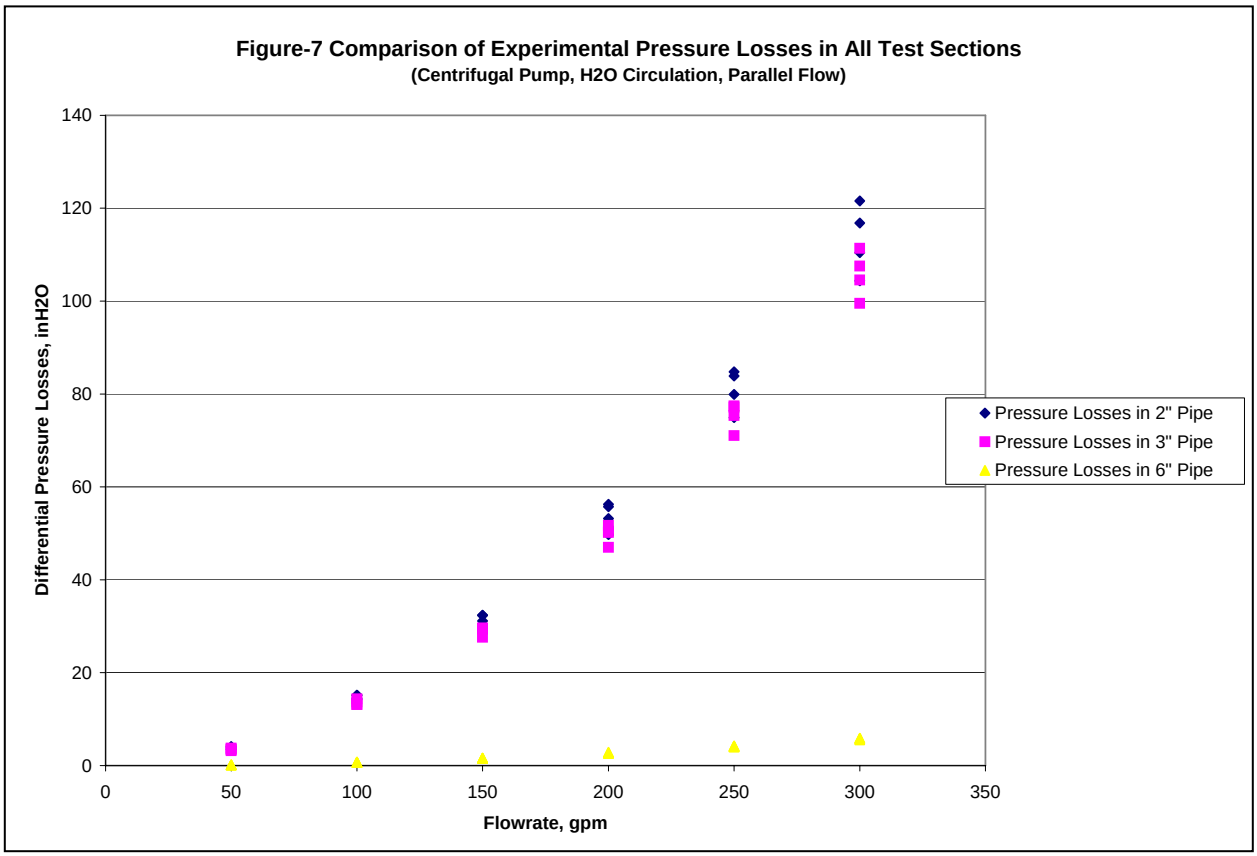
Figure-7 Comparison of Experimental Pressure Losses in All Test Sections
(Centrifugal Pump, H2O Circulation, Parallel Flow)
Differential Pressure Losses, inH2O
Flowrate, gpm
0
20
40
60
80
100
120
140
0
50
100
150
200
250
300
350
Pressure Losses in 2" Pipe
Pressure Losses in 3" Pipe
Pressure Losses in 6" Pipe

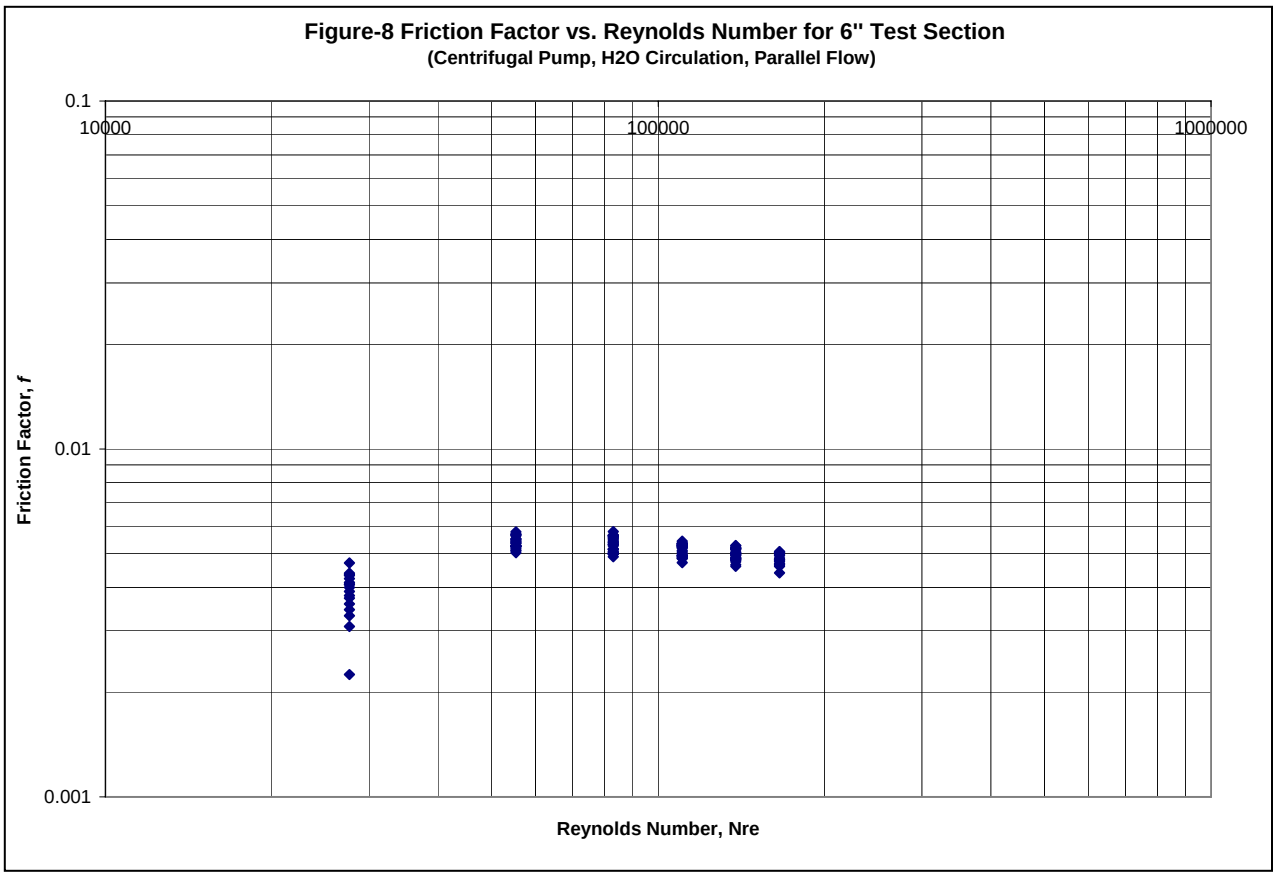
Figure-8 Friction Factor vs. Reynolds Number for 6" Test Section
(Centrifugal Pump, H2O Circulation, Parallel Flow)
Friction Factor, f
Reynolds Number, Nre
0.1
0.01
0.001
10000
100000
1000000

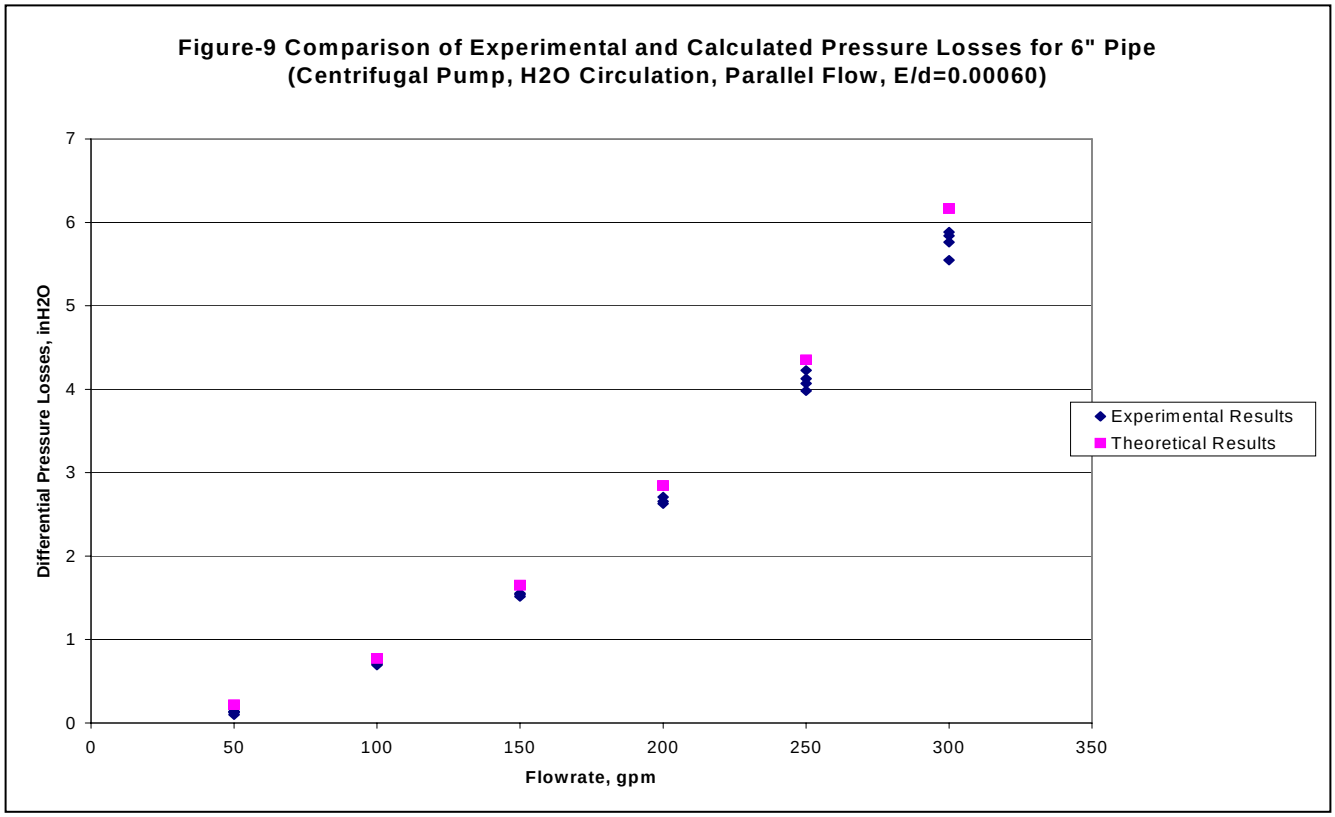
Figure-9 Comparison of Experimental and Calculated Pressure Losses for 6" Pipe
(Centrifugal Pump, H2O Circulation, Parallel Flow, E/d=0.00060)
Differential Pressure Losses, inH2O
Flowrate, gpm
0
1
2
3
4
5
6
7
0
50
100
150
200
250
300
350
Experimental Results
Theoretical Results